

## High Pressure Raman Study of Hexafluorobenzene Crystals

Yoshio Suzuki,<sup>†</sup> Hiroko Shimada,<sup>\*</sup> and Ryoichi Shimada<sup>†</sup>

Department of Chemistry, Faculty of Science, Fukuoka University, Nanakuma, Jonan-ku, Fukuoka 814-80

<sup>†</sup>Department of Electronics, Faculty of Technology, Fukuoka Institute of Technology,  
Wajiro-Higashi, Higashi-ku, Fukuoka 811-02

(Received May 29, 1996)

Pressure effects on the Raman active inter- and intramolecular vibrations of hexafluorobenzene crystals were studied under hydrostatic pressures up to about 5 GPa at room temperature in a gasketed diamond anvil cell. The observed Raman spectra indicate that very gradual application of pressure to hexafluorobenzene liquid up to about 0.3 GPa gives rise to supercompressed liquid and the supercompressed liquid crystallizes in phase I by further successive applications of pressure. On the other hand, hexafluorobenzene liquid crystallizes in phase II by quick application of pressure up to about 0.8 GPa. The crystal structure in phase I grown via supercompression is unchanged up to about 2–4 GPa, depending on the experimental conditions and finally transfers to phase II. Coexistence of the crystal phases I and II gives complex spectral structures in both the inter- and intramolecular vibrational regions under various pressures. The pressure-induced frequency shift of the intermolecular vibrations of hexafluorobenzene crystal is compared with those of hexachloro- and hexabromobenzene crystals and it is shown that the repulsive force between the bromine atoms belonging to different molecules is stronger than the repulsive forces between the fluorine atoms and also between the chlorine atoms.

The Raman spectra of benzene and hexachlorobenzene crystals observed under high pressure were studied by several workers and they showed that a benzene crystal undergoes phase transitions under 1.4 and 2.7 GPa,<sup>1–3)</sup> while no phase transition takes place in a hexachlorobenzene crystal up to 5 GPa.<sup>4)</sup> Borden et al.<sup>5)</sup> studied the crystal structure of hexafluorobenzene by X-ray diffraction and showed that the crystal structure resembles to a hexachlorobenzene crystal rather than a benzene crystal. Recently, Shimada et al. observed pressure effects on the Raman bands due to the intermolecular vibrations of 1,2,4,5-tetrachloro-<sup>6)</sup> and 1,2,4,5-tetrabromobenzene<sup>7)</sup> crystals and discussed the intermolecular repulsive forces between the bromine atoms and between the chloride atoms. They also studied the temperature effects on the intermolecular vibrations of a hexabromobenzene crystal.<sup>8)</sup>

Abramowitz and Levin<sup>9)</sup> and Laposa and Montgomery<sup>10)</sup> gave the assignment of the normal vibrations of fluorobenzene through analyses by the Raman and infrared spectra. Very recently Suzuki et al.<sup>11)</sup> reinvestigated the assignment of the normal vibrations of fluorobenzene through the normal coordinate calculation. Shimada et al. calculated the pressure-induced frequency shift of the intramolecular vibrations of several halo-substituted benzene crystals.<sup>4,6,7)</sup>

In this work, the Raman active inter- and intramolecular vibrations of a hexafluorobenzene crystal are studied under high pressure and the pressure-induced phase transition and the pressure-induced intramolecular vibrational frequency shift are discussed.

### Experimental

**Materials.** Hexafluorobenzene obtained from Tokyo Kasei

Chem. Inc. was purified by repeated vacuum distillations.

**Optical Measurement.** The Raman spectra of a hexafluorobenzene crystal due to the inter- and intramolecular vibrations were measured with a JEOL 400T laser Raman spectrophotometer and Bio-Rad FT-Raman II NBR-9001 under various pressures from 1 atm ( $1 \times 10^{-4}$  GPa) to 5 GPa at room temperature by the backscattering observation method. The 514.5 and 476.5 nm beams from an Ar<sup>+</sup> ion laser of Spectra Physics and 1064 nm beam from a Nd:YAG laser of Spectra Physics were used for the excitation. A diamond anvil cell obtained from Toshiba Tungaloy Co. was used for measurement of the Raman spectrum under high pressure. The method of observation of the Raman spectrum is exactly the same as described previously.<sup>6,7)</sup> Pressure was applied by two different processes. In the first case the pressure was applied at the rate of about 0.1 GPa from 1 atm to 1 GPa until the hexafluorobenzene liquid crystallized completely. In the second case the pressure was applied quickly up to 0.8 GPa, under which the hexafluorobenzene liquid crystallized quickly. In both processes the sample was left overnight after pressure was applied to the sample. The first and second processes are referred to as the gradual and quick application of pressure hereafter, respectively. The pressure inside the gasket hole was measured by the wavelength shift of the R<sub>1</sub> fluorescence line at 694.2 nm emitted from ruby chips, using the equation proposed by Mao et al.<sup>12)</sup> The pressure inside the hole was confirmed to be hydrostatic by observing the shapes of the R<sub>1</sub> and R<sub>2</sub> (692.7 nm) fluorescence lines emitted from the ruby.

### Results and Discussion

#### Temperature Effects on the Intermolecular Vibrations.

The melting point of hexafluorobenzene is 5 °C under 1 atm. The crystal structure of hexafluorobenzene at 120 K belongs to the monoclinic space group  $P2_1/n$  ( $C_{2h}^5$ ) with six molecules in the unit cell; four of these molecules are

in the general positions (Wyckoff position e) and two in the special positions at the centers of symmetry (Wyckoff position c).<sup>5)</sup> According to the group theory the eighteen rotational intermolecular vibrations are Raman active and these vibrations are classified into symmetry species Ag and Bg, nine vibrations belonging to each species.

The Raman spectra of a hexafluorobenzene crystal in the intermolecular vibrational region observed at various temperatures under 1 atm are shown in Fig. 1 (A) and the temperature-frequency curves are given in Fig. 1 (B). Figure 1 indicates that (1) five bands (a, b, c, d, e) could be observed in the spectra among the eighteen Raman active bands, (2) the spectral structure was unchanged with decreasing temperature except for the fact that a shoulder band was resolved in the higher frequency side of the band a, and (3) the slope of the temperature-frequency curves increased monotonically and continuously with decreasing temperature. These observed facts indicate that no phase transition took place in the hexafluorobenzene crystal in the temperature range from 5 to  $-196^\circ\text{C}$ . The crystal phase observed in this temperature range is referred to as phase I.

#### Pressure Effects on the Intermolecular Vibrations.

The Raman spectra due to the intermolecular vibrations of the hexafluorobenzene crystals observed under various pressures are shown in Fig. 2 (A) and (B). The spectra shown in Fig. 2 (A) were observed when pressure was applied very slowly and the spectra shown in Fig. 2 (B) were observed when pressure was applied very quickly up to 0.8 GPa. The observed spectra indicate that the hexafluorobenzene crystal grew through two different crystallization processes depending on the application of pressure. The two different crystallization processes could be clearly distinguished under polarized microscope. When pressure was applied to liquid

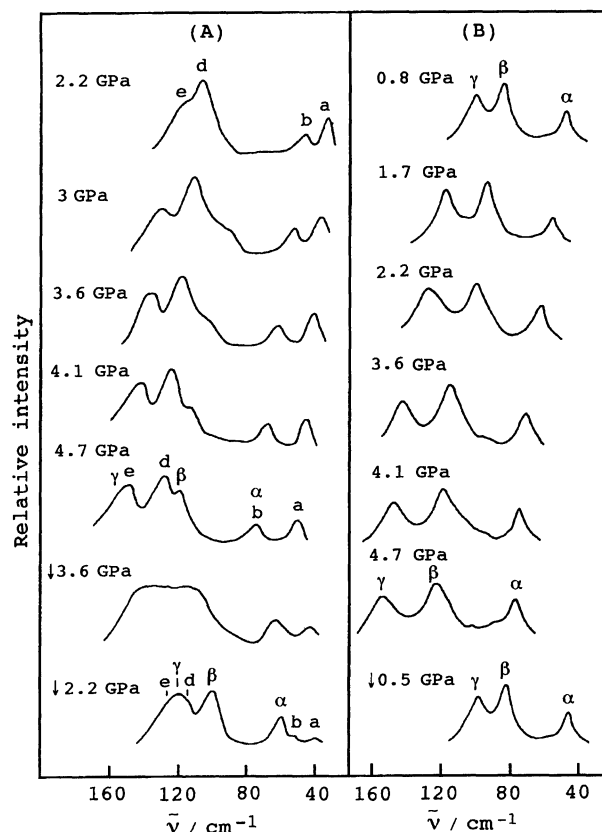


Fig. 2. The Raman spectra of the hexafluorobenzene crystals in the intermolecular vibrational region observed under various pressures at room temperature. (A) and (B) refer to the spectra observed applying pressure slowly and quickly, respectively.

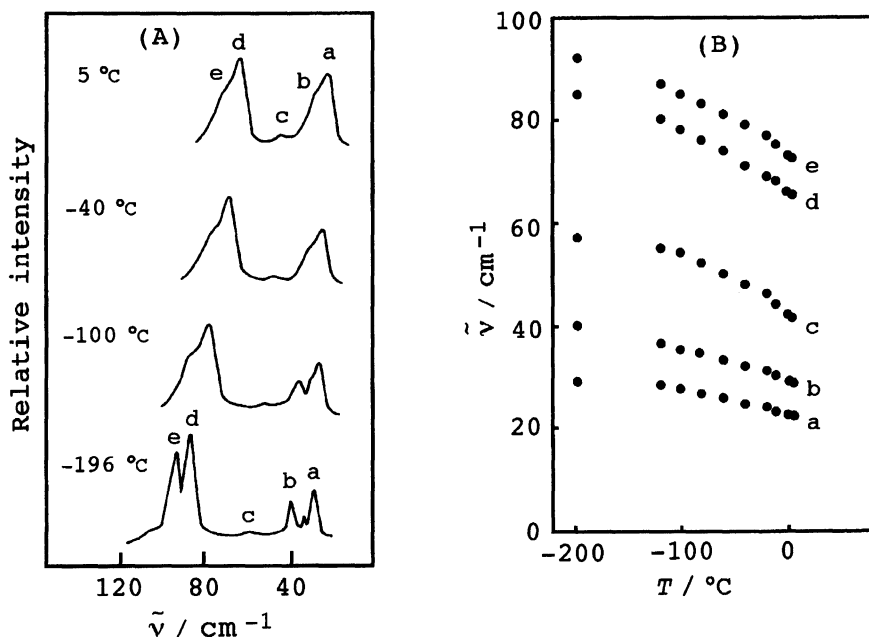


Fig. 1. The Raman spectra (A) and the temperature-frequency curves (B) of the hexafluorobenzene crystals in the intermolecular vibrational region observed at various temperatures under 1 atm.

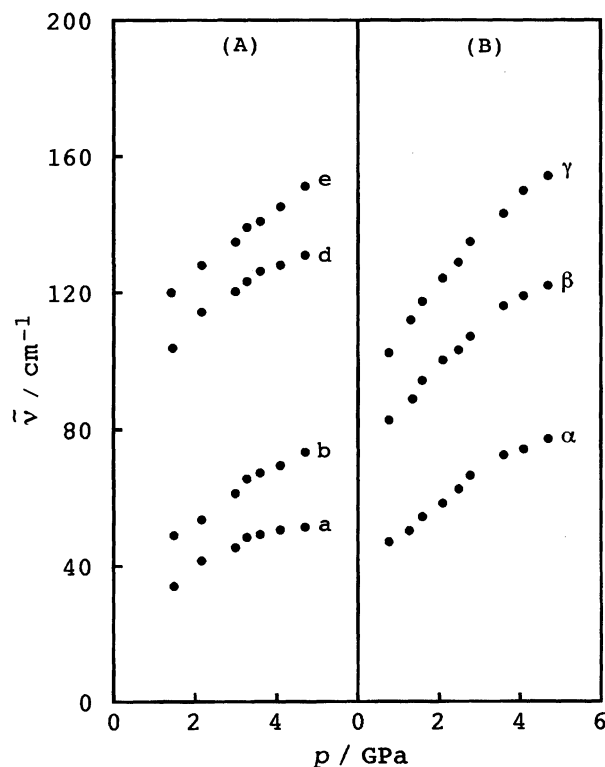


Fig. 3. Pressure-frequency curves of the Raman bands of the hexafluorobenzene crystals in the intermolecular vibrational region observed at room temperature. (A) and (B) refer to the curves obtained applying pressure slowly and quickly, respectively. One atm corresponds to  $10^{-4}$  GPa ( $\approx 0$  GPa).

very slowly up to about 0.3 GPa, a dendrite phenomenon was observed under polarized microscope, just as generally seen in semiconductors in the supercooled condition.

This observation suggests that the hexafluorobenzene liquid with this dendrite nature is in the supercompressed state. The supercompressed liquid crystallized by successive application of pressure up to about 1 GPa. The Raman spectrum of the crystal grown via supercompression observed under 2.2 GPa is shown at the top of the Fig. 2 (A). The spectral structure is the same as that observed in the phase I as described in the temperature effect, except for the fact that the band c could not be resolved because of its very weak intensity. This fact indicates that the crystal grown via supercompression exists in phase I. The spectral structure observed in phase I was almost completely preserved with increasing pressure up to about 3 GPa and then became fairly complex as can be seen in the spectrum observed under 4.7 GPa shown in Fig. 2 (A). When the pressure was decreased from 4.7 GPa, the spectrum lost the structure under  $\downarrow 3.6$  GPa, where the sign  $\downarrow$  indicates the decrease of pressure, and the spectrum under  $\downarrow 2.2$  GPa mainly consisted of three bands.

The spectrum of the quickly crystallized sample observed under 0.8 GPa consisted of three bands ( $\alpha$ ,  $\beta$ ,  $\gamma$ ) and the spectral structure was quite different from that observed in phase I. The spectral structure was unchanged with increasing pressure up to 4.7 GPa and also with decreasing pressure from 4.7 GPa to 0.5 GPa. When pressure was further de-

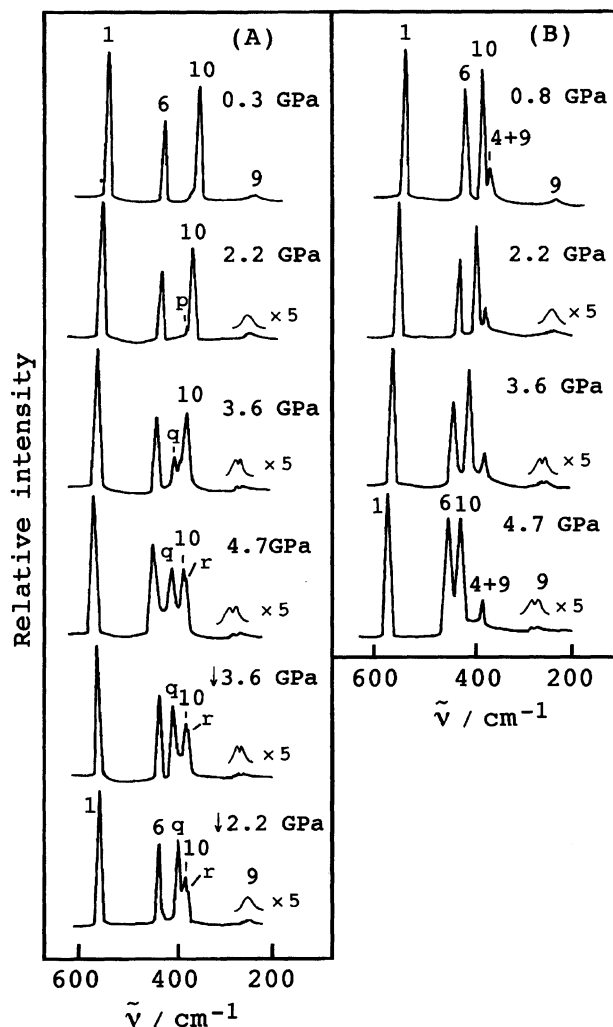


Fig. 4. The Raman spectra of the hexafluorobenzene crystals in the intramolecular vibrational region observed under various pressures at room temperature. (A) and (B) refer to the spectra observed applying pressure slowly and quickly, respectively.

creased from 0.5 GPa, the crystal liquefied. The crystal phase giving three band structure is referred to as phase II.

The pressure-frequency curves obtained from Fig. 2 (A) and (B) are shown in Fig. 3 and (A) and (B), respectively. Figure 3 (A) and (B) show that the frequencies of the bands  $\alpha$ ,  $\beta$ , and  $\gamma$  in phase I and the frequencies of the bands  $\alpha$ ,  $\beta$ , and  $\gamma$  in phase II increased gradually and continuously with increasing pressure. The frequencies of the bands marked  $\alpha$ ,  $\beta$ , and  $\gamma$  in Fig. 2 (A) under 4.7 GPa coincided with the frequencies of the bands  $\alpha$ ,  $\beta$ , and  $\gamma$  observed under 4.7 GPa in Fig. 2 (B), respectively. In Fig. 2 (A) the spectral structure observed under 2.2 GPa with increasing pressure and the structure under  $\downarrow 2.2$  GPa with decreasing pressure were quite different. The frequencies of the bands  $\alpha$ ,  $\beta$ , and  $\gamma$  under  $\downarrow 2.2$  GPa were equal to the frequencies of the bands  $\alpha$ ,  $\beta$ , and  $\gamma$  observed under 2.2 GPa in Fig. 2 (B), respectively.

These observations suggest that the spectra observed under

Table 1. Raman Frequency of the Intermolecular Vibrations of the Hexafluorobenzene Crystals

		1 atm		
		5 °C	−100 °C	−196 °C
	Band	$\tilde{\nu}/\text{cm}^{-1}$	$\tilde{\nu}/\text{cm}^{-1}$	$\tilde{\nu}/\text{cm}^{-1}$
Phase I	a	22	28	29
	b	28	35	40
	c	40	54	57
	d	64	78	85
	e	72	85	92
		Room temperature		
	Band	2.2 GPa	3.6 GPa	4.7 GPa
		$\tilde{\nu}/\text{cm}^{-1}$	$\tilde{\nu}/\text{cm}^{-1}$	$\tilde{\nu}/\text{cm}^{-1}$
Phase I	a	41	49	51
	b	53	67	73
	d	114	126	131
	e	128	141	151
		Room temperature		
	Band	0.8 GPa	2.2 GPa	4.7 GPa
		$\tilde{\nu}/\text{cm}^{-1}$	$\tilde{\nu}/\text{cm}^{-1}$	$\tilde{\nu}/\text{cm}^{-1}$
Phase II	$\alpha$	47	60	77
	$\beta$	83	100	122
	$\gamma$	102	125	154

Table 2. Frequency of the Intramolecular Vibrations of the Hexafluorobenzene Crystals

		1 atm		
		5 °C	−100 °C	−196 °C
	Band	$\tilde{\nu}/\text{cm}^{-1}$	$\tilde{\nu}/\text{cm}^{-1}$	$\tilde{\nu}/\text{cm}^{-1}$
Phase I	$\nu_9$	265	268	271
	$\nu_{10}$	373	376	379
	$\nu_6$	445	446	448
	$\nu_1$	561	562	564
		Room temperature		
	Band	2.2 GPa	3.6 GPa	4.7 GPa
		$\tilde{\nu}/\text{cm}^{-1}$	$\tilde{\nu}/\text{cm}^{-1}$	$\tilde{\nu}/\text{cm}^{-1}$
Phase I	$\nu_{9e}^a)$		280	284
		274		
	$\nu_{9c}^a)$		285	293
	$\nu_{10}$	386	395	400
	$\nu_6$	453	458	461
	$\nu_1$	572	581	585
		Room temperature		
	Band	0.8 GPa	2.2 GPa	4.7 GPa
		$\tilde{\nu}/\text{cm}^{-1}$	$\tilde{\nu}/\text{cm}^{-1}$	$\tilde{\nu}/\text{cm}^{-1}$
Phase II	$\nu_{9e}^a)$			285
		269	274	
	$\nu_{9c}^a)$			295
	$\nu_{10}$	394	408	433
	$\nu_6$	448	453	460
	$\nu_1$	565	577	589

a) e and c refer to the vibrations of molecules located at the Wyckoff e and c sites, respectively.

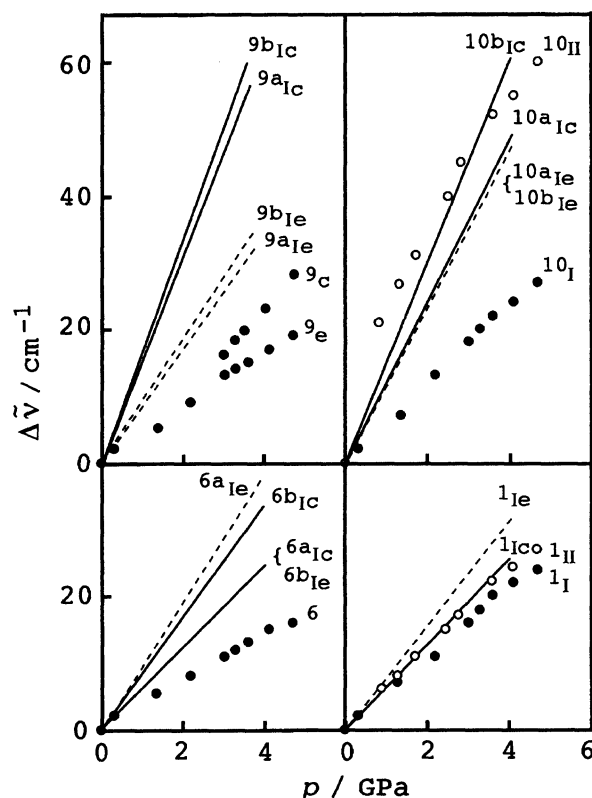


Fig. 5. Pressure-frequency shift curves of the Raman bands in the intramolecular vibrational region. ●●● and ○○○ refer to the curves obtained in the phases I and II, respectively. The subscripts I and II refer to the phases I and II, respectively. — and --- refer to the calculated pressure-frequency shift curves for the molecules located at the Wyckoff c and e sites in the phase I, respectively. The values of  $\Delta\tilde{\nu} = \Delta\tilde{\nu}_{p \text{ GPa}} - \Delta\tilde{\nu}_{1 \text{ atm}}$  are plotted in the ordinate.

4.7 and ↓2.2 GPa in Fig. 2 (A) are a mixture of the bands due to the crystal phases I and II. The intensities of the bands a, b, d, and e decreased, while the intensities of the bands,  $\alpha$ ,  $\beta$ , and  $\gamma$  increased with decreasing pressure from 4.7 to 2.2 GPa, as can be seen in Fig. 2 (A). The spectral structures observed under 3, 3.6, 4.1, and ↓3.6 GPa shown in Fig. 2 (A) are well explained by the mixture of the bands due to the crystal phases I and II. These results indicate that (1) the crystal phase I was obtained via supercompression and the crystal transferred to phase II after supercompression was broken, and (2) phase I may exist in a very narrow pressure region at room temperature. The frequencies of intermolecular vibrations observed under various pressures at room temperature are given in Table 1.

#### Pressure Effects on the Intramolecular Vibrations.

The Raman spectra of the hexafluorobenzene crystal in the intramolecular vibrational region observed under various pressures are shown in Fig. 4 (A) and (B), where (A) and (B) refer to the spectra observed for the crystal grown slowly via supercompression (phase I) and the crystal grown quickly (phase II), respectively. In these figures the Raman bands assigned to the fundamental  $\nu_9$ ,  $\nu_{10}$ ,  $\nu_6$ , and  $\nu_1$  vibrations and the combination vibration of  $\nu_4 + \nu_9$  are given.<sup>11)</sup> The fre-

Table 3. Calculated Pressure-Induced Frequency Shift of the Intramolecular Vibrations of the Hexafluorobenzene Crystals in Phase I

Band	$\tilde{\nu}_p \text{ GPa} - \tilde{\nu}_1 \text{ atm}$					
	Wyckoff c			Wyckoff e		
	1 GPa $\tilde{\nu}/\text{cm}^{-1}$	2 GPa $\tilde{\nu}/\text{cm}^{-1}$	4 GPa $\tilde{\nu}/\text{cm}^{-1}$	1 GPa $\tilde{\nu}/\text{cm}^{-1}$	2 GPa $\tilde{\nu}/\text{cm}^{-1}$	4 GPa $\tilde{\nu}/\text{cm}^{-1}$
$\nu_{9a}$	16	31	66	9	16	33
$\nu_{9b}$	18	34	71	10	18	37
$\nu_{10a}$	15	26	48	14	25	46
$\nu_{10b}$	18	32	58	14	25	46
$\nu_{6a}$	6	11	25	10	19	41
$\nu_{6b}$	8	16	33	6	12	25
$\nu_1$	6	12	26	8	15	33

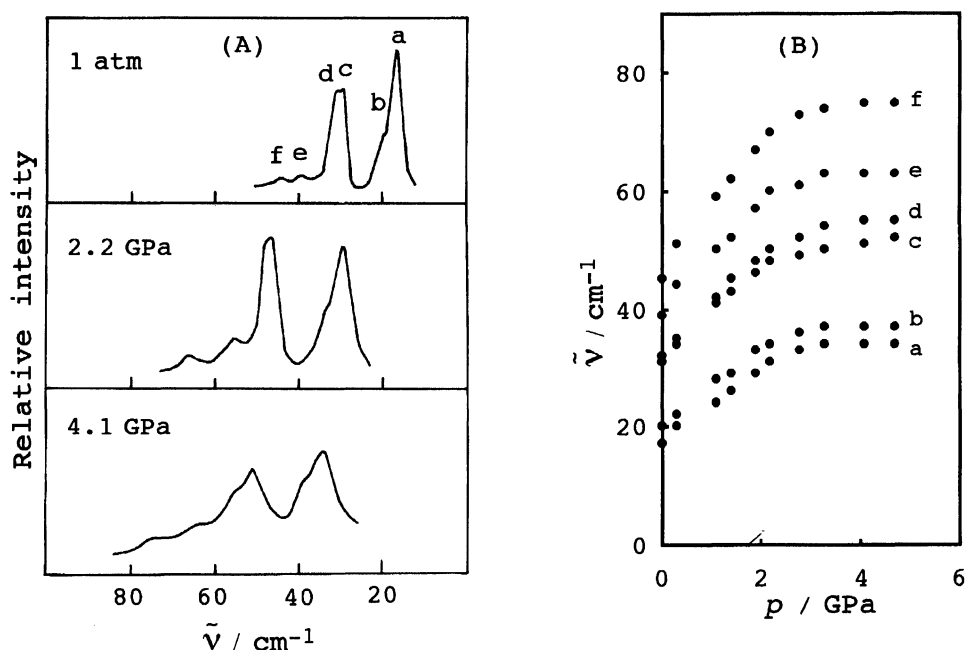


Fig. 6. The Raman spectra (A) and the pressure–frequency curves (B) of the hexabromobenzene crystals in the intermolecular vibrational region observed under various pressures at room temperature.

Table 4. Raman Frequencies of the Intermolecular Vibrations of the Hexabromo- and Hexachlorobenzene Crystals

Band	Hexabromobenzene			Hexachlorobenzene <sup>a)</sup>		
	1 atm $\tilde{\nu}/\text{cm}^{-1}$	2.8 GPa $\tilde{\nu}/\text{cm}^{-1}$	4.7 GPa $\tilde{\nu}/\text{cm}^{-1}$	1 atm $\tilde{\nu}/\text{cm}^{-1}$	2.8 GPa $\tilde{\nu}/\text{cm}^{-1}$	4.7 GPa $\tilde{\nu}/\text{cm}^{-1}$
a	17	33	34	20	46	56
b	20	36	37	23	46	54
c	31	49	52	37	74	84
d	32	52	55	43	74	82
e	39	61	63	52	91	98
f	45	73	75	55		

a) Taken from Ref. 4.

quencies of the four fundamental vibrations observed under various conditions are given in Table 2. The spectral structure observed in phase II shown in Fig. 4 (B) was unchanged by application of pressure, while the spectral structure ob-

served in phase I shown in Fig. 4 (A) changed markedly by application of pressure just as observed in the case of the intermolecular vibrations. In Fig. 4 (A) the intensity of the band assigned to the  $\nu_{10}$  vibration decreased and a new

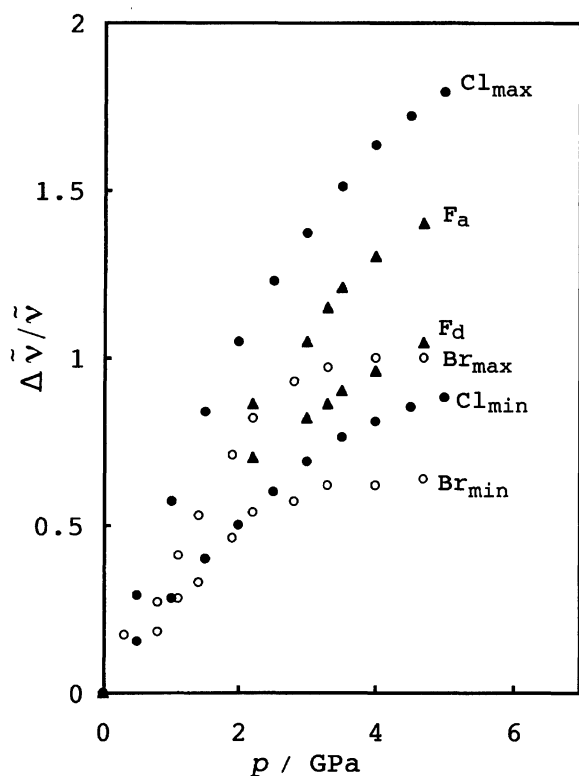


Fig. 7. Pressure effect on the maximum and minimum values of  $\Delta\tilde{\nu}/\tilde{\nu}$  among the six values for the intermolecular vibrational Raman bands of the hexachlorobenzene (●●●) and hexabromobenzene (○○○) crystals. Pressure effect on the values of  $\Delta\tilde{\nu}/\tilde{\nu}$  for the intermolecular vibrational Raman bands a and d of the hexafluorobenzene crystals (▲▲▲). The values of  $\Delta\tilde{\nu}/\tilde{\nu}$  are defined as  $(\tilde{\nu}_p \text{ GPa} - \tilde{\nu}_1 \text{ atm})/\tilde{\nu}_1 \text{ atm}$ .

band marked q appeared with higher intensity with increasing pressure up to 4.7 GPa, and the relationship between the intensities of the  $\nu_{10}$  and q bands increased with decreasing pressure from 4.7 GPa. The band marked r was also clearly resolved with decreasing pressure from 4.7 GPa. The frequencies of the bands q and r shown in Fig. 4 (A) are equal to the frequencies of the  $\nu_{10}$  and  $\nu_4 + \nu_9$  combination vibrations under the same pressure in Fig. 4 (B), respectively.

These phenomena are well explained in the same way as described for the pressure effect on the intermolecular vibrations. It is concluded that the spectrum under 0.3 GPa shown in Fig. 4 (A) is due to the supercompressed liquid and the spectrum under 2.2 GPa is due to phase I crystallized via supercompression. The spectra under 3.6, 4.7, ↓3.6, and ↓2.2 GPa shown in Fig. 4 (A) are due to the coexisting phases I and II. It is quite clear that the spectra under 2.2 and ↓2.2 GPa in Fig. 4 (A) are different, because the former spectrum is ascribed to phase I crystallized via supercompression, while the latter is ascribed to phases I and II coexisting due to the break of the supercompression. Therefore, the bands q and r are reasonably ascribed to the bands due to the  $\nu_{10}$  and  $\nu_4 + \nu_9$  vibrations in the phase II, respectively.

The band assigned to the  $\nu_9$  vibration became wide with increasing pressure and split into two bands under above

3 GPa in both phases I and II. The splitting of the band may be due to the site group splitting of the  $\nu_9$  vibration of molecules located in the different Wyckoff sites e and c but not to the splitting of  $\nu_9$  mode into the  $\nu_{9a}$  and  $\nu_{9b}$  modes as shown by the calculation of the pressure-induced frequency shift described below. The weak band marked p in Fig. 4 (A) was assigned to the combination band of the  $\nu_{16}$  and  $\nu_{18}$  vibrations of the  $e_{1g}$  species.

The observed curves of the pressure-frequency shift for the  $\nu_9$ ,  $\nu_{10}$ ,  $\nu_6$ , and  $\nu_1$  vibrations in phases I (●●●) and II (○○○) are given in Fig. 5, which shows that (1) in phases I and II the observed frequency shifts increased monotonically with increasing pressure at the rate of 5–20  $\text{cm}^{-1}/\text{GPa}$  depending on the vibrational modes, (2) the observed frequency shifts for the  $\nu_9$  and  $\nu_6$  vibrations in phase I were almost equal to the shifts in phase II, respectively, (3) the shift for the  $\nu_1$  vibration in phase II was slightly larger than the shift in phase I, (3) the shift for the  $\nu_{10}$  vibration in phase II was much larger than the shift in phase I, and (4) the band due to the  $\nu_9$  vibration split into two bands with increasing pressure in both phases I and II.

The frequency shift of the intramolecular vibrations induced by the intermolecular interactions with the twenty neighboring molecules was calculated, changing the intermolecular distance, which was converted into pressure in the way described previously.<sup>6,7)</sup> The compressibility of the hexafluorobenzene crystal was not available and thus the compressibility was assumed to be the same as that of the hexamethylbenzene crystal.<sup>13)</sup> The parameter of the intermolecular potential was taken from the data given by Spackman.<sup>14)</sup> The calculated pressure-induced frequency shifts,  $\Delta\tilde{\nu} = \tilde{\nu}_p \text{ GPa} - \tilde{\nu}_1 \text{ atm}$ , in the phase I are given in Fig. 5, together with the observed shifts and in Table 3. In Fig. 5, — and --- refer to the calculated curves for the molecules located at the Wyckoff c and e sites in phase I, respectively.

The calculated results gave larger pressure-induced frequency shifts than the observed results, especially for the vibrations involving the displacements of the fluorine atoms. The calculation may be improved by a more desirable choice of the parameters of the intermolecular potential and by use of the compressibility obtained experimentally instead of the assumed one. Although the calculation did not give satisfactory agreement between the calculated and observed frequency shifts, the calculation gives the following interesting results that (1) the repulsive intermolecular force plays a predominant role in the pressure-induced frequency shift compared with the other forces such as the dispersive force, (2) the splittings of the a and b modes of the  $\nu_{10}$  and  $\nu_6$  vibrations were larger than the splitting of the a and b modes of the  $\nu_9$  vibration, except for the  $\nu_{10}$  vibration of the molecule located at the site e, where the splitting of the a and b modes was hardly recognized, (3) the site group splitting of the  $\nu_9$  vibration of the molecules located at the sites c and e was much larger than the site group splittings of the  $\nu_{10}$ ,  $\nu_6$ , and  $\nu_1$  vibrations, and (4) the site group splitting of the  $\nu_9$  vibration was much larger than the splittings of the a and b modes of the  $\nu_{10}$ ,  $\nu_6$ , and  $\nu_9$  vibrations. These results may lead to

the conclusion that the observed splitting for the  $\nu_9$  vibration under high pressure was due to the site group splitting.

**Comparison of the Pressure Effects on the Intermolecular Vibrations in Hexafluoro-, Hexachloro-, and Hexabromobenzene Crystals.** Hexabromobenzene crystallizes in the monoclinic space group  $P2_1/n$  ( $C_{2h}^5$ ) with two molecules in the unit cell.<sup>15)</sup> There are six Raman active intermolecular rotational vibrations and the six vibrations were studied in the previous work for the temperature effect on the Raman active intermolecular vibrations.<sup>8)</sup> The Raman spectra due to the intermolecular vibrations of the hexabromobenzene crystal observed under various pressures are shown in Fig. 6 (A) and the pressure–frequency curves are given in Fig. 6 (B). Six bands (a, b, c, d, e, f) were resolved as shown in Fig. 6 (A). The slopes,  $d\tilde{\nu}/dp$ , of the six pressure–frequency curves increased with increasing pressure up to about 3 GPa and the slopes became gentle and nearly flat under pressures from about 3 to 5 GPa. The unchanged spectral structure and continuous pressure–frequency curve under pressure up to 5 GPa suggest that no phase transition took place in the hexabromobenzene crystal up to 5 GPa. The frequencies of the intermolecular vibrations of the hexabromobenzene crystal are listed in Table 4 together with the frequencies for the hexachlorobenzene crystal.<sup>4)</sup>

To compare the intermolecular forces acting on the pressure-induced intermolecular vibrational frequency shifts in the hexafluoro-, hexachloro-, and hexabromobenzene crystals, the values of  $\Delta\tilde{\nu}/\tilde{\nu}_{1\text{ atm}}$ , where  $\Delta\tilde{\nu}$  refers to  $\tilde{\nu}_p - \tilde{\nu}_{1\text{ atm}}$ , are plotted in Fig. 7. In the hexachloro- and hexabromobenzene crystals, the maximum and minimum values of  $\Delta\tilde{\nu}/\tilde{\nu}_{1\text{ atm}}$  among the six values for the intermolecular vibrational bands are plotted. In the hexafluorobenzene crystal only four intermolecular vibrational bands were clearly detected under various pressures among the eighteen intermolecular vibrational bands and the values of  $\Delta\tilde{\nu}/\tilde{\nu}_{1\text{ atm}}$  for the bands a and d are plotted.

As can be seen in Fig. 7, the slopes of  $\Delta\tilde{\nu}/\tilde{\nu}_{1\text{ atm}}$  for the hexafluoro- and hexachloro-, and hexabromobenzene crystals increased steeply with increasing pressure up to about 3 GPa. The slopes for the hexafluoro- and hexachlorobenzene crystals successively increased, although the slopes became gradually gentle compared with the slopes obtained up to 3 GPa, with increasing pressure, while in the hexabromobenzene crystal the slopes became almost flat under above 3 GPa.

The pressure-induced frequency shift of the intermolecular vibrations is caused by the anharmonic potential and by the change of the equilibrium intermolecular distance due to the change of the compressibility of the crystal by pressure. Vaidya and Kennedy<sup>13)</sup> observed the compressibility of various molecular organic crystals under pressures up to 4.5 GPa and found that the compressibility decreases with increasing molecular volume and the compressibility of the hexabromobenzene crystal is smaller than that of the hexachlorobenzene crystal. It might be expected that the compressibility of the hexabromobenzene crystal is also smaller than the compressibility of the hexafluorobenzene crystal be-

cause the molecular volume of hexafluorobenzene is smaller than that of hexabromobenzene, although the compressibility of the hexafluorobenzene crystal was not reported.

Comparing the compressibilities of these three hexahalobenzene crystals, it can be supposed that the rate of decrement of the intermolecular distance between the neighboring molecules in the hexabromobenzene crystal with increasing pressure was smaller than those in the hexafluoro- and hexachlorobenzene crystals. This consideration could be ascertained by the observation that (1) the value of  $\Delta\tilde{\nu}/\tilde{\nu}_{1\text{ atm}}$  for the hexabromobenzene crystal was smaller than the values for the hexafluoro- and hexachlorobenzene crystals and (2) the value of  $\Delta\tilde{\nu}/\tilde{\nu}_{1\text{ atm}}$  for the hexabromobenzene crystal under above 3 GPa became flat, although the values of  $\Delta\tilde{\nu}/\tilde{\nu}_{1\text{ atm}}$  for the hexafluoro- and hexachlorobenzene crystals increased with increasing pressure above 3 GPa as described above.

The difference of the anharmonic potential in the hexafluoro-, hexachloro-, and hexabromobenzene crystals should also give different contribution to the frequency shift. The contribution of the anharmonic potential to the frequency shift can be estimated if overtone vibrations can be observed.

In conclusion, the study of pressure effects on the Raman bands due to the inter- and intramolecular vibrations of the hexafluorobenzene crystal gives the following results. (1) Hexafluorobenzene crystallized in phase I at 5 °C under 1 atm and no temperature-induced phase transition took place down to –196 °C under 1 atm. (2) Hexafluorobenzene crystallized in phase I via supercompression by applying pressure very gradually and the crystal phase I transferred to the crystal phase II by changing pressure. (3) When hexafluorobenzene was crystallized quickly by applying pressure of 0.8 GPa, hexafluorobenzene crystallized in phase II, where the crystal structure was stable under pressures from about 0.5 to 5 GPa. (4) These phenomena were also ascertained by the fact that the frequency of the  $\nu_{10}$  vibration observed in phase I was different from that observed in phase II. (4) The repulsive force in the hexabromobenzene crystals was stronger than those in the hexafluoro- and hexachlorobenzene crystals.

The authors thank the Japan Private School Promotion Foundation for Science Research Promotion Fund. The authors are grateful to Mr. H. Kawano for his assistance in the calculation of the pressure-induced frequency shift.

## References

- 1) D. M. Adams and R. Appleby, *Proc. R. Soc. London, Ser. A*, **296**, 1896 (1977).
- 2) W. D. Ellenson and M. Nicol, *J. Chem. Phys.*, **61**, 1380 (1974).
- 3) M.-M. Thiéry, K. Kobashi, and I. L. Spain, *Solid State Commun.*, **54**, 95 (1985).
- 4) G. Sadakuni, M. Maehara, H. Kawano, Y. Nibu, H. Shimada, and R. Shimada, *Bull. Chem. Soc. Jpn.*, **67**, 1593 (1994).
- 5) N. Boden, P. P. Davis, C. H. Stam, and G. A. Wesseling, *Mol. Phys.*, **25**, 81 (1973).
- 6) S. Matsukuma, H. Kawano, Y. Nibu, H. Shimada, and R.

Shimada, *Bull. Chem. Soc. Jpn.*, **67**, 1588 (1994).

7) F. Simizu, Y. Suzuki, K. Mitarai, M. Fujino, H. Kawano, Y. Nibu, H. Shimada, and R. Shimada, *Bull. Chem. Soc. Jpn.*, **68**, 1883 (1995).

8) Y. Suzuki, R. Shimada, and H. Shimada, *Res. Bull. Fukuoka Inst. Technol.*, **28**, 31 (1995).

9) S. Abramowitz and I. W. Levin, *Spectrochim. Acta, Part A*, **26A**, 2261 (1970).

10) J. D. Laposa and C. Montgomery, *Spectrochim. Acta, Part*

*A*, **38A**, 1109 (1982).

11) Y. Suzuki, R. Shimada, and H. Shimada, *Res. Bull. Fukuoka Inst. Technol.*, in press.

12) H. K. Mao, P. M. Bell, J. W. Shaner, and D. J. Steinberg, *J. Appl. Phys.*, **49**, 3276 (1978).

13) S. N. Vaidya and G. C. Kennedy, *J. Chem. Phys.*, **55**, 987 (1971).

14) M. A. Spackman, *J. Chem. Phys.*, **85**, 6579 (1986).

15) E. Baharie and G. S. Pawley, *Acta Crystallogr., Sect. A*, **A35**, 233 (1979).

---